Stem Cell Reports
Article

ISSCR

OPEN ACCESS

Astrocytes modulate neurodegenerative phenotypes associated with glaucoma in OPTN(E50K) human stem cell-derived retinal ganglion cells

Cátia Gomes,[1,2,6] Kirstin B. VanderWall,[2,3,6] Yanling Pan,[2,3] Xiaoyu Lu,[1] Sailee S. Lavekar,[2,3] Kang-Chieh Huang,[2,3] Clarisse M. Fligor,[2,3] Jade Harkin,[2,4] Chi Zhang,[1] Theodore R. Cummins,[2,3] and Jason S. Meyer[1,2,4,5,7,*]

[1]Department of Medical and Molecular Genetics, Indiana University School of Medicine, Indianapolis, IN, USA
[2]Stark Neurosciences Research Institute, Indiana University School of Medicine, Indianapolis, IN, USA
[3]Department of Biology, Indiana University Purdue University Indianapolis, Indianapolis, IN, USA
[4]Department of Pharmacology and Toxicology, Indiana University School of Medicine, Indianapolis, IN, USA
[5]Department of Ophthalmology, Glick Eye Institute, Indiana University School of Medicine, Indianapolis, IN, USA
[6]These authors contributed equally
[7]Twitter: @meyerlab
*Correspondence: meyerjas@iu.edu
https://doi.org/10.1016/j.stemcr.2022.05.006

SUMMARY

Although the degeneration of retinal ganglion cells (RGCs) is a primary characteristic of glaucoma, astrocytes also contribute to their neurodegeneration in disease states. Although studies often explore cell-autonomous aspects of RGC neurodegeneration, a more comprehensive model of glaucoma should take into consideration interactions between astrocytes and RGCs. To explore this concept, RGCs and astrocytes were differentiated from human pluripotent stem cells (hPSCs) with a glaucoma-associated OPTN(E50K) mutation along with corresponding isogenic controls. Initial results indicated significant changes in OPTN(E50K) astrocytes, including evidence of autophagy dysfunction. Subsequently, co-culture experiments demonstrated that OPTN(E50K) astrocytes led to neurodegenerative properties in otherwise healthy RGCs, while healthy astrocytes rescued some neurodegenerative features in OPTN(E50K) RGCs. These results are the first to identify disease phenotypes in OPTN(E50K) astrocytes, including how their modulation of RGCs is affected. Moreover, these results support the concept that astrocytes could offer a promising target for therapeutic intervention in glaucoma.

INTRODUCTION

Astrocytes are the most prevalent cell type in the CNS, providing essential support for neurons through a variety of mechanisms, including neurotrophic support, maintenance of the blood-brain barrier, reuptake of neurotransmitter, and synapse modulation, among many other functions (Paixao and Klein, 2010; Sofroniew and Vinters, 2010). Astrocyte support for neurons is essential for the maintenance of homeostasis within the CNS, yet a number of neurodegenerative disorders are associated with astrocyte dysfunction in which astrocytes either fail to provide support for neurons or actively contribute to the neurodegenerative process through the production of neurotoxic compounds (Escartin et al., 2021; Liddelow and Barres, 2017; Phatnani and Maniatis, 2015). As such, astrocytes can also play pivotal roles in the degenerative process.

Glaucoma is a neurodegenerative disease of the retina and optic nerve in which retinal ganglion cells (RGCs) are damaged and subsequently degenerate, resulting in the loss of vision or blindness (Hartwick, 2001; Quigley, 2011). Although cell-autonomous mechanisms result in the degeneration of RGCs (Buckingham et al., 2008; Chitranshi et al., 2018), astrocytes also contribute to the degenerative processes observed in glaucoma in a non-cell-autonomous manner (Cooper et al., 2020; Guttenplan et al., 2020; Shinozaki and Koizumi, 2021). However, although much of what we know about astrocyte modulation of RGCs in glaucoma is due to studies using rodent models, important differences exist between rodents and humans, including a low degree of conservation of both RGCs as well as astrocytes (Hodge et al., 2019; Oberheim et al., 2009; Peng et al., 2019; Zhang et al., 2016b). Human pluripotent stem cells (hPSCs) provide an advantageous model system to better reflect the interactions between astrocytes and RGCs in the human system. Although previous studies have demonstrated the *in vitro* modeling of neurodegenerative features of glaucoma using hPSCs in a cell-autonomous fashion (Ohlemacher et al., 2016; Sharma et al., 2017; Teotia et al., 2017; VanderWall et al., 2020), and astrocytes have been shown to enhance the growth and maturation of hPSC-derived RGCs (VanderWall et al., 2019), studies have not explored the interactions between hPSC-derived astrocytes and RGCs from a glaucoma patient background to examine how astrocytes contribute to the neurodegenerative state.

To address this shortcoming, in the present study we focused upon the differentiation of astrocytes derived from glaucoma OPTN(E50K) hPSCs or isogenic control lines, as well as how astrocytes derived from these populations modulated RGC phenotypes. Significant differences were observed in glaucoma hPSC-derived astrocytes compared

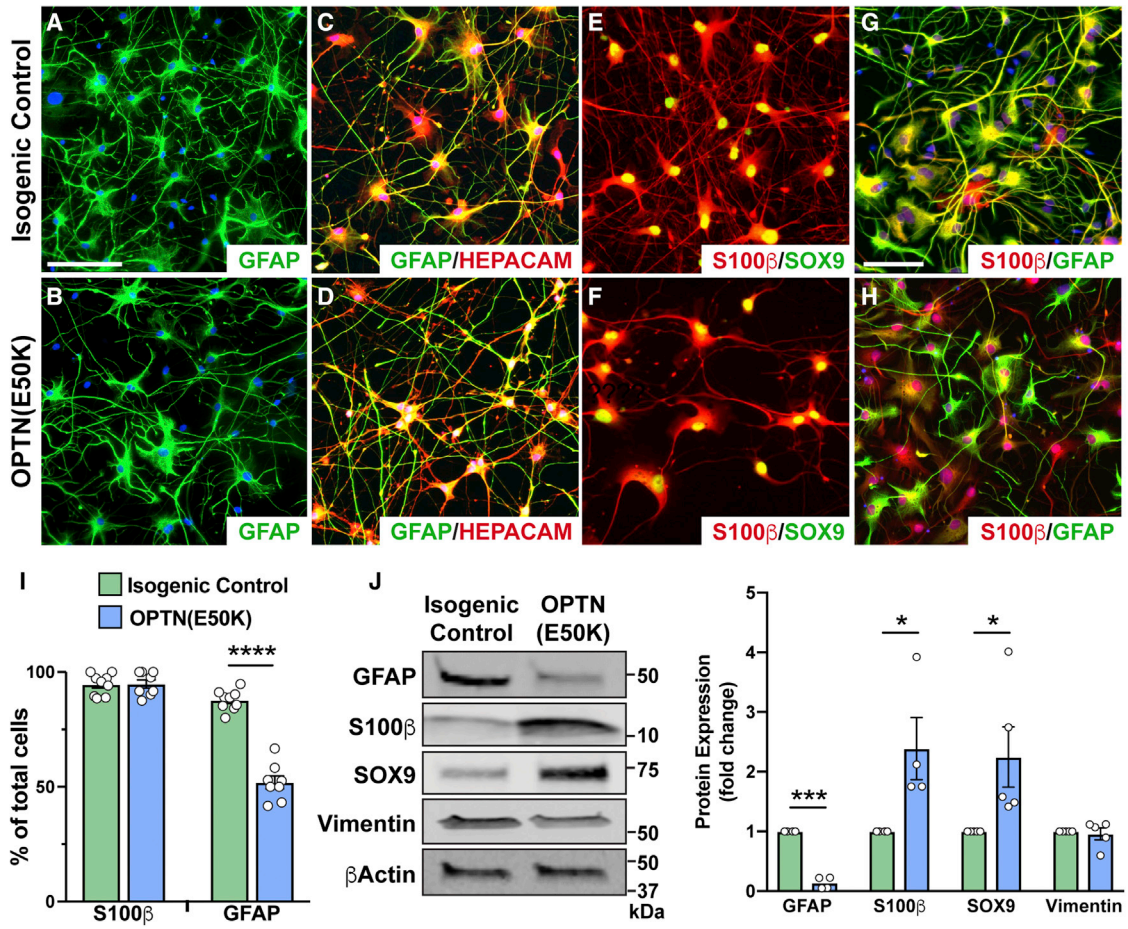

Figure 1. Astrocyte differentiation from isogenic control and OPTN(E50K) hPSCs

(A–F) Astrocytes were differentiated from both cell sources in high purity, and resulting astrocytes expressed a variety of associated markers.

(G–I) Compared with isogenic control astrocytes, a smaller percentage of OPTN(E50K) astrocytes expressed GFAP.

(J) Western blot analyses confirmed a significant decrease in GFAP expression, as well as increased expression of S100β and SOX9.

n = 4 separate differentiation experiments each using H7 and H7(E50K) hPSCs. Scale bars, 100 μm. Error bars represent SEM. *p < 0.05, ***p < 0.001, and ****p < 0.0001.

with isogenic controls, including alterations in characteristic astrocyte-associated protein expression and deficits in the autophagy pathway. The co-culture of hPSC-derived astrocytes resulted in profound effects upon RGCs, with glaucoma astrocytes inducing neurodegenerative phenotypes in RGCs including phenotypic changes and increased excitability. Conversely, the co-culture with healthy astrocytes rescued degenerative phenotypes from glaucoma RGCs. At least some of these astrocyte-derived effects were due to astrocyte-derived secreted factors, as glaucoma astrocyte-conditioned medium conferred degenerative phenotypes upon RGCs. The present study is the first of its kind to identify disease-related phenotypes in glaucoma hPSC-derived astrocytes, as well as to study the interactions of these cells with RGCs in an *in vitro* co-culture paradigm, providing evidence that astrocytes could offer a promising opportunity for neuroprotection in glaucoma.

RESULTS

Neurodegenerative features of OPTN(E50K) astrocytes

Although astrocytes play critical roles in the support of neurons in homeostatic conditions (Sofroniew and Vinters, 2010), various disease states result in profound changes to astrocyte features (Escartin et al., 2021; Phatnani and Maniatis, 2015). Thus, initial efforts focused upon the identification of disease-related changes to astrocytes with a glaucoma OPTN(E50K) mutation compared with isogenic control astrocytes (Figures 1 and S1). To pursue these studies, we used multiple independent cell lines

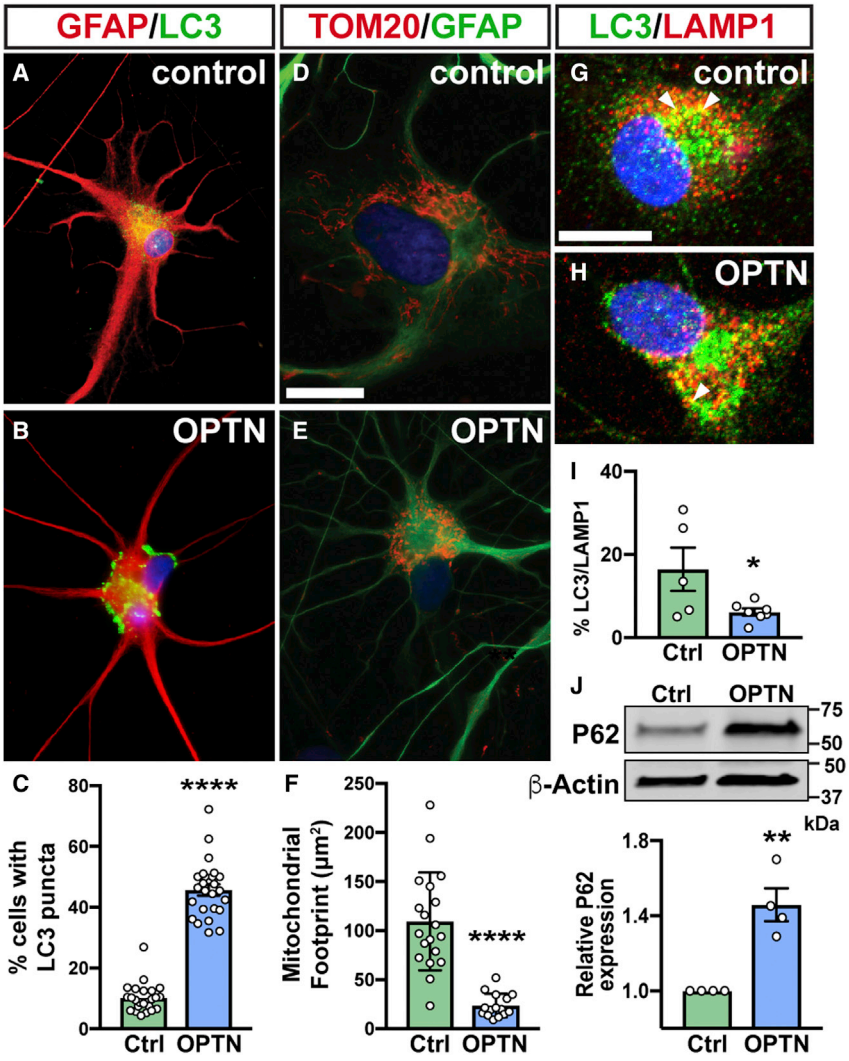

Figure 2. Disease-related features of OPTN(E50K) astrocytes

(A–C) Isogenic control astrocytes demonstrated widespread expression of LC3, while OPTN(E50K) astrocytes displayed significant aggregation of LC3 within the soma.

(D–F) Mitochondria identified by TOM20 immunostaining were observed to be widespread and elongated in isogenic control astrocytes, while OPTN(E50K) astrocytes displayed condensed mitochondria aggregated within the perinuclear region.

(G–I) OPTN(E50K) astrocytes displayed significantly less co-localization of LC3 and LAMP1, suggesting an inability of the autophagosome to fuse with the lysosome.

(J) OPTN(E50K) astrocytes also expressed significantly higher levels of the autophagy-related p62 protein, suggesting autophagy impairment.

n = 3 separate differentiation experiments each using H7 and H7(E50K) hPSCs. A minimum of 5 individual cells from each of at least 3 separate differentiation experiments were used for analysis in (A)–(I). Scale bars, 25 μm (A, B, D, and E) and 10 μm (G and H). Error bars represent SEM. *p < 0.05, **p < 0.01, and ****p < 0.0001.

either with or without the OPTN(E50K) glaucoma-associated mutation, including both patient-derived and CRISPR-Cas9-introduced mutations, along with relevant isogenic controls, as previously described (VanderWall et al., 2020). Astrocytes were efficiently derived from both OPTN(E50K) and isogenic control sources and expressed characteristic markers (Figures 1A–1H). As previous studies have demonstrated changes in the expression of GFAP in disease states (Diaz-Amarilla et al., 2011; Gomes et al., 2019; Yoshii et al., 2011), an analysis of OPTN(E50K) glaucoma astrocytes indicated a decrease in GFAP expression (Figure 1J), with significantly fewer S100β-positive astrocytes co-expressing GFAP (Figures 1G–1J). Full gel images demonstrated the specificity of antibodies used, as well as the absence of other splice variants (Figure S2). Interestingly, this decrease in GFAP expression among OPTN(E50K) astrocytes was also associated with a decrease in proliferation identified by the expression of Ki-67 (Figure S3). Additionally, increased expression of S100β and SOX9 was observed in OPTN(E50K) astrocytes (Figure 1J), similar to previous descriptions for other disease-associated astrocytes (Michetti et al., 2019; Sun et al., 2017).

As the OPTN protein serves a primary role as an autophagy receptor, and deficits in the autophagy and mitochondrial pathways have been previously associated with the OPTN(E50K) mutation (Inagaki et al., 2018; Minegishi et al., 2013; Shim et al., 2016), additional analyses focused on autophagy-related phenotypes (Figures 2 and S1). Although the localization of the autophagy-associated protein LC3 was diffuse within isogenic control astrocytes, a profound aggregation of LC3 protein was observed associated with glaucoma OPTN(E50K) astrocytes (Figures 2A–2C). Additionally, an analysis of mitochondria within astrocytes revealed a compaction of mitochondria in a

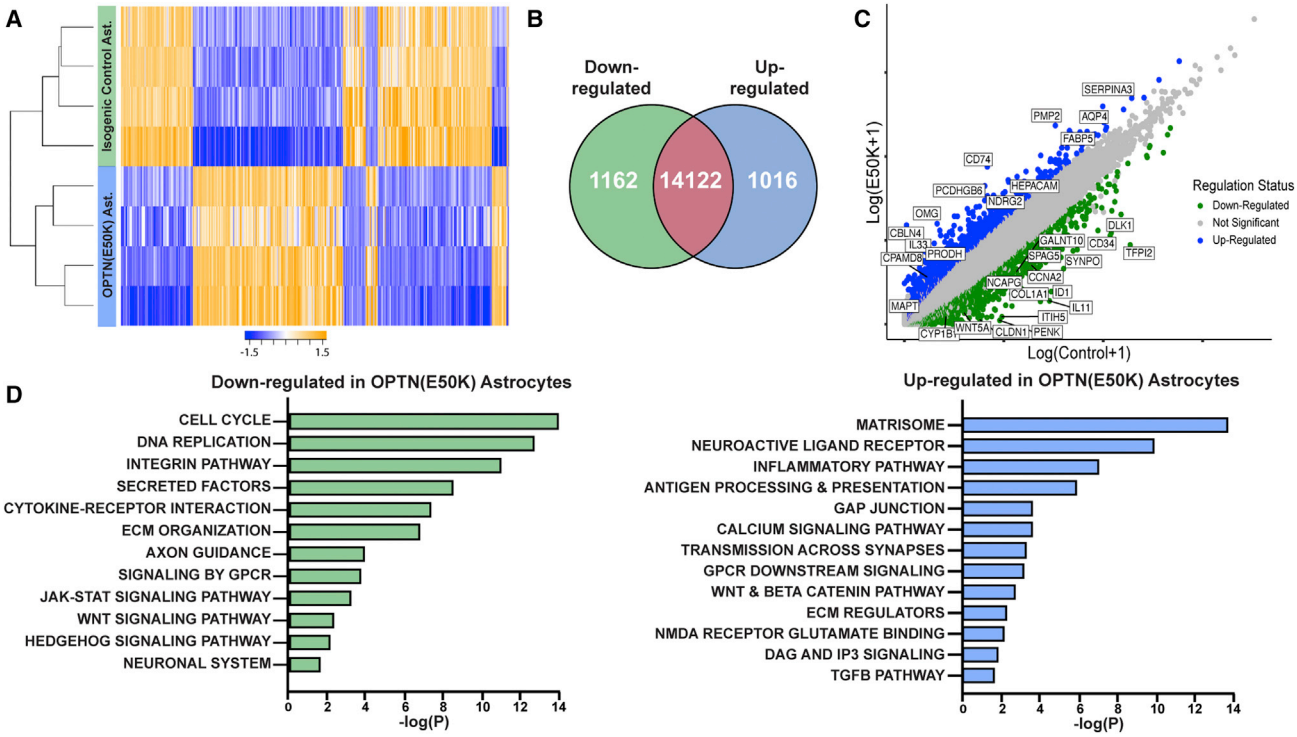

Figure 3. RNA-seq analyses of OPTN(E50K) and isogenic control astrocytes

(A) Heatmap representation of differentially expressed genes between OPTN(E50K) and isogenic control astrocytes. Each row represents one sample, and each column represents one gene. The up- and down-regulated genes are yellow and blue colored, respectively.

(B and C) Venn diagram (B) and (C) scatterplot of differentially expressed genes.

(D) Gene Ontology (GO) and pathway terms from differential gene expression analysis of OPTN(E50K) and isogenic control astrocytes. Statistical significance (−log[p] value on the x axis) was assessed using hypergeometric test.

n = 4 separate differentiation experiments each using H7 and H7(E50K) hPSCs.

perinuclear fashion within OPTN(E50K) astrocytes, resulting in a significantly decreased mitochondrial footprint within these cells (Figures 2D–2F). The localization of LC3 protein indicative of autophagosomes was then compared with the lysosomal protein LAMP1. Compared with isogenic control astrocytes, co-localization of these proteins was significantly decreased in OPTN(E50K) astrocytes (Figures 2G–2I), suggesting dysfunctional autophagy processing. Further dysfunction of the autophagy pathway was observed as a significant increase in the expression of p62 in glaucoma OPTN(E50K) astrocytes (Figure 2J).

Given the numerous phenotypic differences due to the glaucoma OPTN(E50K) mutation, RNA sequencing (RNA-seq) analyses revealed numerous genes differentially expressed in astrocytes from OPTN(E50K) or isogenic control sources, including astrocyte-associated markers HEPACAM and Aquaporin-4, as well as genes that are associated with neurodegeneration, including MAPT and the glaucoma-associated CYP1B1 (Sena et al., 2004; Zhang et al., 2016a) (Figures 3A–3C). Pathway enrichment analyses identified numerous cellular pathways that were differentially modulated because of the OPTN(E50K) glaucoma mutation ($p < 0.05$, hypergeometric test), with OPTN(E50K) astrocytes downregulating genes associated with the cell cycle and DNA replication ($p < 1e\text{-}6$), while upregulating genes associated with pathways including the matrisome, inflammatory pathway, and gap junctions, among others ($p < 1e\text{-}4$, Figure 3D).

Astrocytes modulate RGC structure and function

Although astrocytes provide critical support to RGCs to maintain homeostasis (VanderWall et al., 2019; Vecino et al., 2016), they can also be toxic to RGCs and significantly contribute to the degeneration of these cells (Cooper et al., 2020; Guttenplan et al., 2020). Thus, to explore the possibility that astrocytes with the OPTN(E50K) mutation contribute to neurodegeneration, co-cultures were established to identify morphological changes to RGCs due to either glaucoma OPTN(E50K) or healthy isogenic control astrocytes. Both isogenic control and OPTN(E50K) cell lines effectively differentiated into RGCs expressing characteristic morphologies and molecular markers (Figure S4),

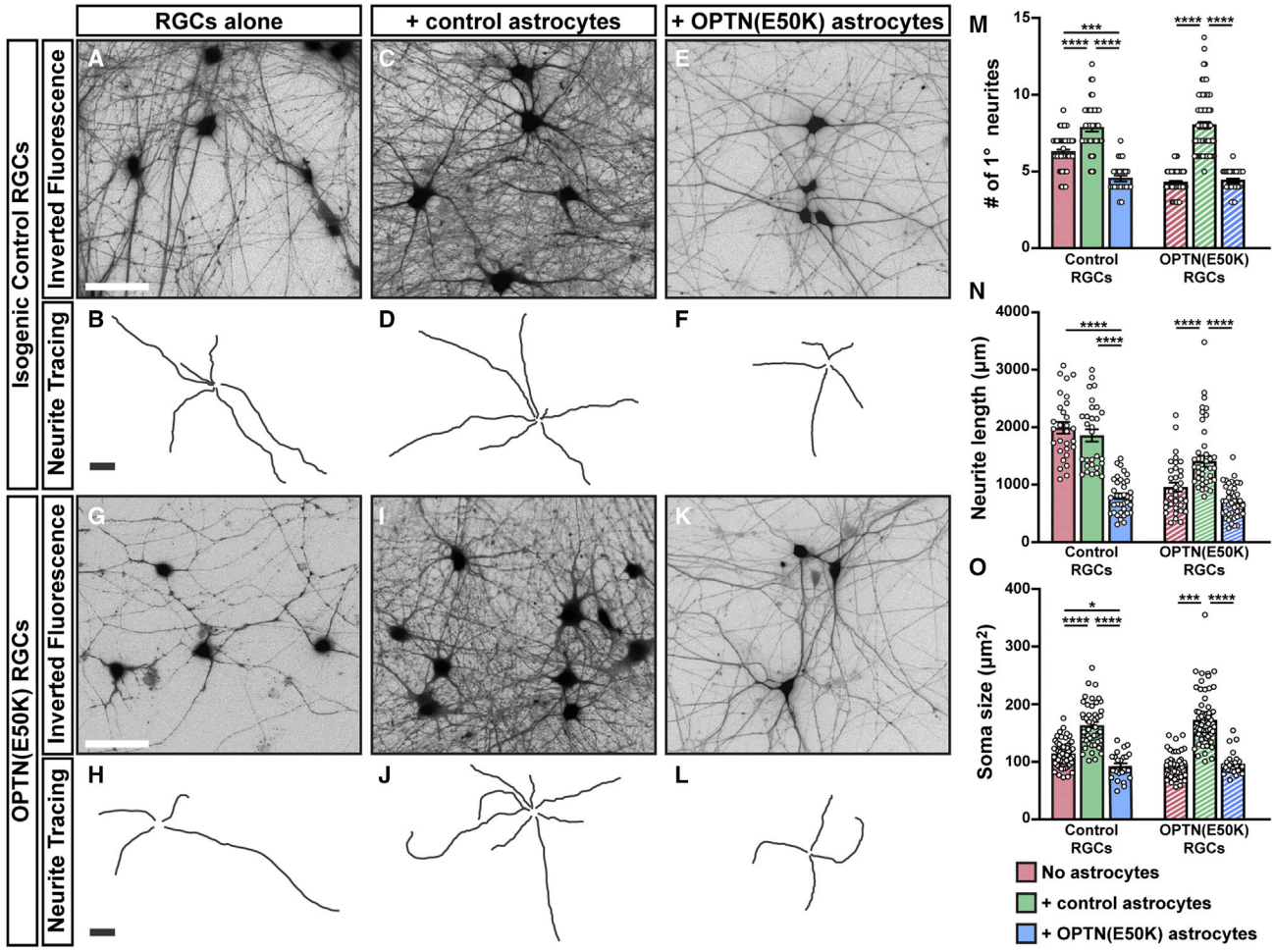

Figure 4. Astrocytes modulate RGC phenotypes

(A–F) Compared with isogenic control RGCs grown alone, those grown in the presence of healthy isogenic control astrocytes exhibit enhanced neurite outgrowth, while those grown in the presence of OPTN(E50K) astrocytes exhibit a reduction of primary neurites as well as soma size.

(G–L) OPTN(E50K) RGCs exhibit degenerative phenotypes that can be rescued in the presence of healthy isogenic control astrocytes, whereas OPTN(E50K) astrocytes did not have an observable effect.

(M–O) Quantification of results from these co-culture assays.

$n \geq 3$ separate differentiation experiments each using H7 and H7(E50K) hPSCs. A range of 10–15 RGCs were analyzed per condition. Scale bars, 50 µm (white bars refer to A, C, E, G, I, and K) and 100 µm (black bars refer to B, D, F, H, J, and L). Error bars represent SEM. *$p < 0.05$, ***$p < 0.001$, ****$p < 0.0001$.

as we have previously described (Ohlemacher et al., 2016; VanderWall et al., 2019, 2020). After 4 weeks of co-culture, a time point at which we have previously demonstrated significant differences between OPTN(E50K) and isogenic control RGCs grown alone (VanderWall et al., 2020), healthy isogenic control RGCs grown in the presence of healthy astrocytes exhibited increased neurite outgrowth (Figures 4A–4D), similar to previous studies (VanderWall et al., 2019). Conversely, astrocytes with the glaucoma OPTN(E50K) mutation conferred neurodegenerative phenotypes upon otherwise healthy RGCs (Figures 4E and 4F), suggesting an active role for astrocytes in RGC neurodegeneration. Furthermore, although RGCs with the glaucoma OPTN(E50K) mutation grown alone exhibited degenerative phenotypes including reduced neurite length and number (Figures 4G and 4H), their co-culture with healthy isogenic control astrocytes rescued these phenotypes (Figures 4I and 4J), while co-culture with OPTN(E50K) astrocytes did not affect morphological features of OPTN(E50K) RGCs (Figures 4K and 4L).

Next, to determine if the presence of healthy or glaucoma astrocytes affected functional properties of RGCs,

whole-cell patch-clamp analyses were performed on either healthy or glaucoma OPTN(E50K) RGCs grown in culture with either healthy or glaucoma OPTN(E50K) astrocytes. RGCs in all conditions could conduct ionic currents (Figure 5A). However, upon the stimulation of RGCs in current-clamp experiments, elicited action potentials were more frequent when either astrocytes or RGCs possessed the OPTN(E50K) mutation, which was even more pronounced when both RGCs and astrocytes harbored the OPTN(E50K) mutation (Figures 5B and 5C). When the OPTN(E50K) glaucoma mutation was present in one or both cell types in co-culture, significant differences were observed in the RGC sodium current density, input resistance, cellular capacitance, and action potential current threshold (Figures 5D–5G). Furthermore, when co-cultures were established with glaucoma OPTN(E50K) astrocytes, nearly all RGCs were capable of firing evoked action potentials in response to a 1 ms stimulation (Figure 5H). Collectively, these results demonstrate the ability for healthy isogenic control astrocytes to regulate OPTN(E50K) RGC excitability, while RGCs grown with OPTN(E50K) astrocytes exhibited hyperexcitable properties, suggesting that astrocytic regulation of excitotoxic mechanisms may contribute to glaucoma neurodegeneration.

Analysis of astrocyte-derived secreted factors contributing to RGC neurodegenerative phenotypes

Astrocytes modulate neuronal function through either contact-dependent or paracrine mechanisms, and previous studies have demonstrated that diseased astrocytes secrete factors contributing to neuronal degeneration (Ramirez-Jarquin et al., 2017; Tripathi et al., 2017). To examine if secreted factors from isogenic control and OPTN(E50K) astrocytes modulated RGC phenotypes, Transwell co-cultures were established to identify secreted factors that contribute to RGC degenerative phenotypes (Figure 6). Significant differences were observed in the average number of primary neurites as well as the soma size for both isogenic control and OPTN(E50K) RGCs when grown in conditioned medium from OPTN(E50K) astrocytes, suggesting that astrocytes exert at least some effects through the release of soluble factors (Figures 6A–6F). Interestingly, the growth of glaucoma OPTN(E50K) RGCs with conditioned medium from healthy isogenic control astrocytes significantly improved the number of primary neurites, demonstrating the importance of maintaining healthy astrocytes for RGC homeostasis.

Next, to determine if differences were caused by specific secreted factors, a Meso Scale Discovery (MSD) analysis tested for differences in the relative abundance of candidate secreted factors from OPTN(E50K) and isogenic control astrocytes (Figure 6G). Among this panel, healthy isogenic control astrocytes secreted elevated levels of IL-6 and IL-8. Conversely, glaucoma OPTN(E50K) astrocytes did not secrete any of these factors above control levels found in basal medium, suggesting a reduced capacity for these cells to provide trophic support for RGCs. Although RNA-seq analyses demonstrated that isogenic control and OPTN(E50K) cells did not differ in the transcriptional levels of IL-6, subsequent MSD analyses of astrocyte cell lysates demonstrated a decreased production of this protein by OPTN(E50K) astrocytes (relative fold change 9.516 ± 2.154, $p < 0.005$). To test the ability of candidate factors to rescue degenerative phenotypes, IL-6 was exogenously added (50 ng/mL) to OPTN(E50K) RGCs, resulting in a rescue of soma size and a partial recovery of the number of primary neurites (Figures 6H and 6I), with control experiments demonstrating that the exogenous application of IL-6 did not significantly affect healthy isogenic control RGCs (Figure S5). Additionally, the application of exogenous TNF-α, which did not exhibit differential expression, did not result in any discernable effects upon OPTN(E50K) or isogenic control RGCs (Figure S6), supporting the specificity of effects observed due to IL-6. To further confirm that the replacement of missing secreted factors could improve the overall health of OPTN(E50K) RGCs, western blot analyses demonstrated that exogenous IL-6 treatment also increased the expression of synaptic proteins (Figures 6M and 6N).

DISCUSSION

Astrocytes play essential roles in the maintenance of homeostatic conditions for neurons, including RGCs (Sofroniew and Vinters, 2010), yet this support is often compromised in disease states such as glaucoma (Formichella et al., 2014; Guttenplan et al., 2020). Diseased astrocytes can lead to the degeneration of neurons through either neurotoxic mechanisms in which astrocytes secrete toxic substances, or by a lack of support in which neurons are deprived of essential pro-survival factors (Liddelow and Barres, 2017; Phatnani and Maniatis, 2015; Syc-Mazurek and Libby, 2019). In either case, altered interactions between neurons and astrocytes lead to neurodegenerative features. However, the precise mechanisms underlying these changes are varied and remain unclear.

In the present study, profound differences were observed in astrocytes with the OPTN(E50K) mutation when compared with healthy isogenic control astrocytes, including changes in the expression of GFAP, S100β, and SOX9 (Figure 1). Importantly, these differences were consistently observed across multiple cell lines, including paired isogenic lines, ensuring that these differences were due to the OPTN(E50K) mutation rather than variability between cell lines. Interestingly, previous studies have

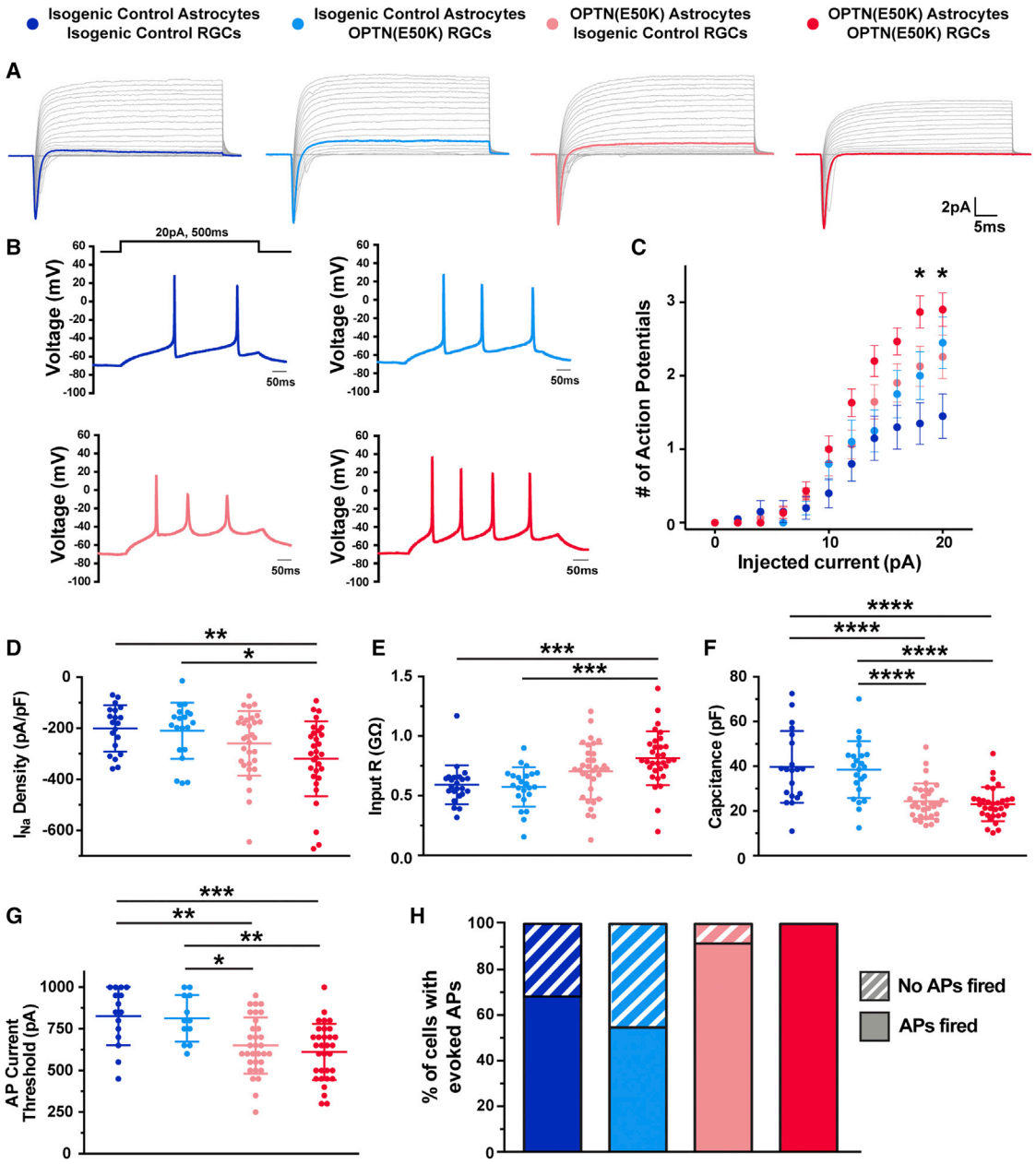

Figure 5. OPTN(E50K) astrocytes confer hyperexcitable profiles to RGCs

(A) Ionic currents recorded from RGCs in the presence of astrocytes in each experimental condition.

(B and C) OPTN(E50K) RGCs grown with OPTN(E50K) astrocytes fired significantly more action potentials upon current injection compared with RGCs in other conditions.

(D–G) RGCs grown with OPTN(E50K) astrocytes resulted in increased sodium current density, increased input resistance, decreased cell capacitance, and decreased action potential threshold.

(H) Following 1 ms current injections, a higher percentage of RGCs on OPTN(E50K) astrocytes fired action potentials compared with RGCs on isogenic control astrocytes.

n = 4 separate differentiation experiments each using H7 and H7(E50K) hPSCs. Error bars represent SEM. *p < 0.05, **p < 0.01, ***p < 0.001, and ****p < 0.0001.

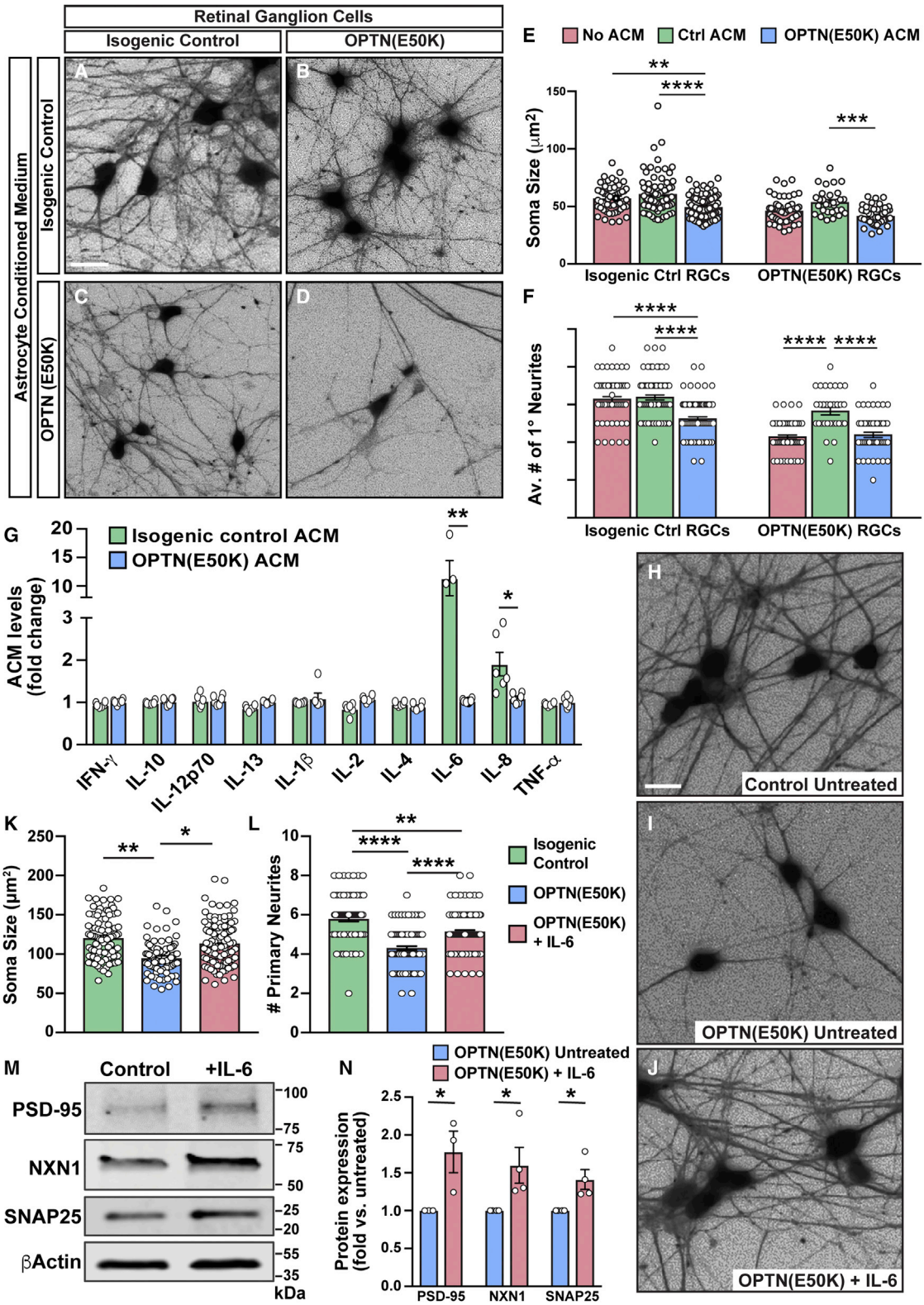

(legend on next page)

associated disease phenotypes in astrocytes with an increase in GFAP expression, particularly in classically reactive astrocytes (Escartin et al., 2021; Hol and Pekny, 2015), rather than a decrease. However, the possibility exists that decreased GFAP expression is indicative of a disease state in which astrocytes fail to provide neuroprotective support. Indeed, previous studies in other systems have similarly demonstrated the decreased expression of GFAP associated with a disease state (Diaz-Amarilla et al., 2011; Gomes et al., 2019; Yoshii et al., 2011), as well as differences in the expression of other astrocyte-associated proteins including SOX9 and S100β (Michetti et al., 2019; Sun et al., 2017).

The OPTN protein plays a primary role as an autophagy receptor (Slowicka et al., 2016), and autophagy dysfunction can be strongly associated with a variety of neurodegenerative diseases (Chu, 2019). Interestingly, an accumulation of the autophagy-related LC3 protein was found within OPTN(E50K) astrocytes, correlated with a condensation of mitochondria within the soma as well as a significantly decreased co-expression of LC3 and LAMP1 (Figure 2), suggesting a decreased ability for the autophagosome to fuse with the lysosome (De Leo et al., 2016). Taken together, these results strongly suggested the potential for astrocyte autophagy dysfunction to be associated with a disease phenotype.

To further assess the functional consequences of the OPTN(E50K) mutation in astrocytes, RNA-seq analysis identified many differentially expressed genes and pathways. Among them, many upregulated genes had been previously associated with neurodegenerative diseases and retinopathies, including SORL1 (Verheijen et al., 2016; Yin et al., 2015), MAPT (Zhang et al., 2016a), and NDP (Ohlmann et al., 2005), further suggesting that an upregulation of these genes in OPTN(E50K) astrocytes could be associated with degenerative phenotypes. Conversely, many downregulated genes in OPTN(E50K) astrocytes have been associated with the cell cycle and proliferation. Interestingly, it was observed that OPTN(E50K) astrocytes grew slower than astrocytes derived from isogenic control cell lines, correlated with a decrease in proliferation on the basis of the expression of Ki-67 (Figure S3). Decreased proliferation is characteristic of cellular senescence (Cohen and Torres, 2019; Gruber et al., 2009), which has been associated with a number of neurodegenerative diseases (Caprioli, 2013; Martinez-Cue and Rueda, 2020), and could thus be a mechanism underlying the neurodegenerative phenotypes observed in this study.

Previous studies in other neurodegenerative diseases such as amyotrophic lateral sclerosis (ALS) have demonstrated that astrocytes can tightly regulate neurodegenerative features in other types of neurons such as motor neurons (Das and Svendsen, 2015; Marchetto et al., 2008; Meyer et al., 2014), yet studies had not previously shown similar features in glaucoma. Interestingly, in the present study, the co-culture of OPTN(E50K) RGCs with healthy isogenic control astrocytes resulted in a significant increase in the number of primary neurites, total neurite length, and soma size. Conversely, the significant reduction in RGC neurite length, branching, and soma size for healthy control RGCs grown in the presence of OPTN(E50K) astrocytes demonstrated that astrocytes could confer disease-related features upon otherwise healthy RGCs. Indeed, neurodegenerative phenotypes were also associated with a "fragmented" appearance of neurites, particularly in OPTN(E50K) RGCs, similar to the fragmentation previously described in other neurodegenerative diseases (Ko et al., 2020). Additionally, as the neurodegenerative effects of astrocytes upon neurons are typically achieved through either contact-dependent mechanisms or via the release of soluble factors that act upon neurons (Phatnani and Maniatis, 2015), significant differences were observed depending on whether RGCs were grown in either control or OPTN(E50K) astrocyte-conditioned medium (ACM). These effects were not as robust as those observed when RGCs were grown in direct contact with astrocytes, suggesting that both contact-dependent and soluble factors are involved in astrocyte-induced neurodegeneration.

Figure 6. Analysis of factors secreted by OPTN(E50K) astrocytes upon RGCs

(A–D) Isogenic control and OPTN(E50K) RGCs expressing BRN3b:tdTomato in the presence of isogenic control and OPTN(E50K) astrocyte-conditioned medium.

(E and F) Quantification of results demonstrated significant effects of astrocyte-conditioned medium upon RGCs, with OPTN(E50K) astrocyte-conditioned medium resulting in degenerative phenotypes compared to isogenic control conditioned medium.

(G) Meso Scale Discovery analysis revealed a reduced secretion of IL-6 and IL-8 from OPTN(E50K) astrocytes compared with isogenic control astrocytes. Values are fold change compared with basal medium alone.

(H–L) Representative inverted fluorescent images of BRN3b:tdTomato RGCs demonstrating a reduction of neuronal complexity due to the OPTN(E50K) mutation, which could be partially rescued following treatment with exogenous IL-6.

(M and N) In response to exogenous treatment with IL-6, OPTN(E50K) RGCs expressed significantly higher levels of synaptic proteins, a measure of RGC health and maturation state.

$n \geq 3$ separate differentiation experiments with at least 15 individual RGCs analyzed for each experiment using H7 and H7(E50K) hPSCs. Scale bars, 30 μm (A–D) and 20 μm (H–J). Error bars represent SEM. *$p < 0.05$, **$p < 0.01$, ***$p < 0.001$, and ****$p < 0.0001$.

Further analyses sought to identify candidate secreted factors that could underly at least some neurodegenerative phenotypes caused by OPTN(E50K) astrocytes, with IL-6 and IL-8 differentially observed within conditioned medium. Although an overproduction of these factors is typically associated with a pro-inflammatory response (Fominykh et al., 2018; Phuagkhaopong et al., 2017), it was interesting that the expression of these factors was significantly decreased from OPTN(E50K) astrocytes. In fact, of all the factors assayed, OPTN(E50K) astrocytes did not secrete any above baseline levels. This lack of secreted factors further supports the concept that OPTN(E50K) astrocytes have not adopted a reactive phenotype, but rather have lost their neurosupportive role for RGCs, similarly leading to neurodegeneration. Supporting the concept of a reduced neurosupportive role, the application of exogenous IL-6 to OPTN(E50K) RGCs resulted in the partial rescue of some neurodegenerative phenotypes. Additionally, these results also demonstrate the diverse roles of secreted factors and the importance of their concentrations. Whereas IL-6 is often discussed as a neurotoxic compound produced by reactive astrocytes (Phuagkhaopong et al., 2017), basal levels of IL-6 are actually essential for neuronal support, with lack of IL-6 leading to RGC apoptosis (Perigolo-Vicente et al., 2013; Sappington et al., 2006). Indeed, the role of IL-6 as either protective or destructive varies depending upon the study and/or conditions analyzed, and the current study suggests a protective role for IL-6. Additionally, it is likely that other factors are also involved in the observed phenotypes beyond the simple role of IL-6. Indeed, the effects of secreted factors upon RGCs in the conditioned medium experiments were not as large as those observed when astrocytes were grown in direct contact with RGCs, suggesting that some contact-dependent mechanisms are involved. Furthermore, although a lack of IL-6 may be responsible for some observed phenotypes, and this may represent a mechanism by which healthy astrocytes confer some degree of neuroprotection upon OPTN(E50K) RGCs, the lack of IL-6 does not necessary explain why OPTN(E50K) astrocytes were capable of conferring disease phenotypes upon otherwise healthy RGCs. In this study, the decreased expression of IL-6 was likely due to changes in the production of the IL-6 protein, rather than transcription of the gene or processes by which the protein is secreted by the cells. Thus, although other factors are clearly involved, the involvement of IL-6 represents an intriguing avenue for further discovery.

Although neurodegeneration can be thought of as a state in which neurons begin to lose their functionality, many studies have demonstrated that degenerating neurons exhibit hyperexcitable properties as an early indicator of dysfunction (Cueva Vargas et al., 2015; Netzahualcoyotzi and Tapia, 2015). Indeed, our previous studies demonstrated that RGCs with the OPTN(E50K) mutation exhibited hyperexcitable properties (VanderWall et al., 2020). In the present study, the presence of the OPTN(E50K) mutation in astrocytes led to an enhanced degree of hyperexcitability, particularly when this gene variant was found within both RGCs and astrocytes. Additionally, when the OPTN(E50K) mutation was present in only one cell type, it appeared to be more consequential when it was present in astrocytes rather than RGCs, with the OPTN(E50K) astrocyte/control RGC condition more similar to the paired OPTN(E50K) astrocytes and RGCs.

Finally, although the OPTN(E50K) mutation is a leading cause of inherited forms of glaucoma (Fan and Wiggs, 2010; Minegishi et al., 2013; Sears et al., 2019), and studies using hPSCs with this mutation are highly informative for a greater understanding of the disease state (VanderWall et al., 2020), current *in vitro* models do not completely reflect the glaucomatous condition within the eye, particularly as it relates to the interactions between astrocytes and RGCs. Although astrocytes are found within the nerve fiber layer of the retina and throughout the optic nerve head and optic nerve (Bussow, 1980), it is typically the astrocytes within the optic nerve head that are associated with an induction of disease-related features within RGC axons as they exit the eye through the lamina cribrosa (Conforti et al., 2007; Mac Nair and Nickells, 2015; Syc-Mazurek and Libby, 2019; Whitmore et al., 2005). In that context, astrocytes typically act in a focal manner upon the axonal compartment of RGCs. Although the present study provides an accurate representation of astrocyte and RGC interactions, particularly how astrocytes can modulate RGC health and induce neurodegenerative properties, it will also be important in future studies to take into consideration the highly compartmentalized nature of RGCs and how glial cells can modulate RGCs in a precise and focal manner.

EXPERIMENTAL PROCEDURES

Maintenance of hPSCs

hPSCs were maintained according to previously described protocols (Fligor et al., 2020; Ohlemacher et al., 2015). Briefly, hPSC colonies were grown on Matrigel-coated 6-well plates in mTeSR1 and passaged using dispase (2 mg/mL) at a 1:6 ratio. Detailed protocols are available in supplemental experimental procedures.

Differentiation of astrocytes and RGCs

hPSCs were differentiated following established protocols to yield either astrocytes (Krencik and Zhang, 2011; VanderWall et al., 2019) or RGCs (Ohlemacher et al., 2016; VanderWall et al., 2020). For RGC differentiation, RGCs were isolated from retinal organoids following enzymatic dissociation and enrichment by

MACS sorting (VanderWall et al., 2019). Detailed protocols are available in supplemental experimental procedures.

Co-culture of hPSC-derived RGCs and astrocytes

Co-cultures of hPSC-derived astrocytes and RGCs were established as previously described (VanderWall et al., 2019), using direct contact or astrocyte-conditioned media. To test astrocyte-derived secreted factors, astrocytes were grown on Transwell culture inserts and placed in the same wells as purified RGCs to create a continuous astrocyte-conditioned media environment. Both direct co-culture and Transwell systems were maintained for 4 weeks before experimental analysis.

Immunocytochemistry

Cells grown on coverslips were fixed in 4% paraformaldehyde for 30 min at room temperature (RT) and then immunostained as previously described (VanderWall et al., 2020). Detailed procedures are provided in supplemental experimental procedures, with a list of primary antibodies used found in Table S1.

Western blot

Protein samples of astrocytes and RGCs were collected in 2% SDS or lysis buffer (M-PER Mammalian Protein Extraction Reagent; Thermo Fisher Scientific), and western blot was performed as described before (VanderWall et al., 2020). Detailed procedures are provided in supplemental experimental procedures, as well as a list of primary antibodies used found in Table S1.

Meso Scale Discovery assay

Astrocyte-conditioned media or cell lysates from isogenic control and OPTN(E50K) astrocytes were collected and analyzed using the Meso Scale Discovery V-Plex Proinflammatory Panel 1 according to the manufacturer's protocol. Following addition of calibrators and samples, the plate was sealed and incubated on a plate shaker for 2 h at RT. Following 3 washes, a prepared antibody solution containing all 10 detection antibodies was added, and the plate was incubated for 2 h at RT. The plate was then washed 3 times with wash buffer, and following the last wash, 2× read buffer was added and the plate was analyzed using the Meso Scale Discovery plate reader.

Quantification and statistical analyses

Isogenic control and OPTN(E50K) astrocytes from a minimum of 3 biological replicates were used in each study. The number of GFAP- and S100β-expressing cells, as well as the percentage of cells containing LC3 puncta, were quantified using the ImageJ cell counter plugin. To quantify the number of LC3 and/or LAMP1 puncta, these features were analyzed with the "analyze particles" option in Fiji, while the mitochondrial footprint within astrocytes was measured using the Mitochondrial Network Analysis (MiNA) tool in Fiji. The co-localization plugin of ImageJ was used to determine the percentage of co-localization between LC3 and LAMP1. Student's *t* test was used to determine significance at a p value < 0.05. For astrocyte-conditioned medium and direct co-culture experiments, BRN3b:tdTomato was imaged to determine morphological properties of RGCs. tdTomato fluorescent images were converted into 8-bit image files using ImageJ (Fiji) software, followed by analysis using the NeuroAnatomy plugin and Simple Neurite Tracer to quantify soma size area, the number of primary neurites, and neurite length. Statistical significance was determined using one-way ANOVA followed by Tukey's post hoc analysis on the basis of a p value < 0.05. Following the Meso Scale Discovery assay, statistical differences in signal averages were determined using one-way ANOVA followed by Tukey's post hoc analysis on the basis of a p value < 0.05. Western blot results were normalized to loading controls and represented as fold change versus isogenic control astrocytes, or untreated RGCs, and Student's *t* test was used to determine statistical differences. In those experiments in which data points were obtained from individual RGCs, data were represented by showing each individual data point. In contrast, when experiments were performed upon entire cell populations, an average from each experiment was taken, and the data represent the average of experimental averages.

RNA sequencing

RNA was collected from astrocytes differentiated as described above using the RNeasy Mini Kit (74104; Qiagen), and total RNA was evaluated for its quantity and quality using an Agilent Bioanalyzer 2100 before preparation for RNA sequencing analysis, as previously described (VanderWall et al., 2020). Detailed protocols are available in supplemental experimental procedures.

Electrophysiological recordings

Whole-cell patch-clamp recordings were performed on RGCs following methods as previously described (VanderWall et al., 2020). Detailed protocols are available in supplemental experimental procedures.

Data and code availability

The RNA-seq experiments reported in this paper have been deposited in the Gene Expression Omnibus database (http://www.ncbi.nlm.nih.gov/geo; GSE173129).

SUPPLEMENTAL INFORMATION

Supplemental information can be found online at https://doi.org/10.1016/j.stemcr.2022.05.006.

AUTHOR CONTRIBUTIONS

C.G., K.B.V., C.Z., T.R.C., and J.S.M. designed the experiments. C.G., K.B.V., Y.P., X.L., S.S.L., K.-C.H., C.M.F., and J.H. performed the experiments. C.G., K.B.V., Y.P., X.L., C.Z., T.R.C., and J.S.M. analyzed results. C.G., K.B.V., and J.S.M. wrote the manuscript. C.G., K.B.V., Y.P., C.Z., T.R.C., and J.S.M. edited and revised the manuscript. C.G., K.B.V., K.-C.H., C.Z., T.R.C., and J.S.M. secured funding associated with this project. C.Z., T.R.C., and J.S.M. supervised experiments detailed in this study.

ACKNOWLEDGMENTS

We would like to thank Dr. Don Zack and Dr. Valentin Sluch for sharing the BRN3b:tdTomato:Thy1.2 vectors used in the previous generation of RGC reporter cell lines. Grant support was provided

by the National Eye Institute (R01EY024984 and R01EY033022 to J.S.M.), the BrightFocus Foundation (G2020369 to J.S.M.), the Glaucoma Research Foundation (to J.S.M.), the Indiana Department of Health Spinal Cord and Brain Injury Research Fund (26343 to J.S.M.), the National Institute for Neurodegenerative Disorders and Stroke (R01NS053422 to T.R.C.), and the National Science Foundation (2047631 to C.Z.). Support for this project was also provided by the Sarah Roush Memorial Fellowship from the Indiana Alzheimer's Disease Center (C.G.). This publication was also made possible with partial support a University Fellowship (K.-C.H.) the Stark Neurosciences Research Institute/Eli Lilly and Co. Neurodegeneration Fellowship (K.-C.H.) and from a predoctoral fellowship award (K.B.V.) from the National Institutes of Health, National Center for Advancing Translational Sciences, Clinical and Translational Sciences Award (UL1TR002529, A. Shekhar, principal investigator [PI]).

CONFLICTS OF INTERESTS

J.S.M. holds a patent regarding the retinal differentiation of human pluripotent stem cells. The authors declare no other competing interests.

Received: September 22, 2021
Revised: May 13, 2022
Accepted: May 16, 2022
Published: June 16, 2022

REFERENCES

Buckingham, B.P., Inman, D.M., Lambert, W., Oglesby, E., Calkins, D.J., Steele, M.R., Vetter, M.L., Marsh-Armstrong, N., and Horner, P.J. (2008). Progressive ganglion cell degeneration precedes neuronal loss in a mouse model of glaucoma. J. Neurosci. *28*, 2735–2744. https://doi.org/10.1523/JNEUROSCI.4443-07.2008.

Bussow, H. (1980). The astrocytes in the retina and optic nerve head of mammals: a special glia for the ganglion cell axons. Cell Tissue Res. *206*, 367–378. https://doi.org/10.1007/BF00237966.

Caprioli, J. (2013). Glaucoma: a disease of early cellular senescence. Invest. Ophthalmol. Vis. Sci. *54*, ORSF60–ORSF67. https://doi.org/10.1167/iovs.13-12716.

Chitranshi, N., Dheer, Y., Abbasi, M., You, Y., Graham, S.L., and Gupta, V. (2018). Glaucoma pathogenesis and neurotrophins: focus on the molecular and genetic basis for therapeutic prospects. Curr. Neuropharmacol. *16*, 1018–1035. https://doi.org/10.2174/1570159X16666180419121247.

Chu, C.T. (2019). Mechanisms of selective autophagy and mitophagy: implications for neurodegenerative diseases. Neurobiol. Dis. *122*, 23–34. https://doi.org/10.1016/j.nbd.2018.07.015.

Cohen, J., and Torres, C. (2019). Astrocyte senescence: evidence and significance. Aging Cell *18*, e12937. https://doi.org/10.1111/acel.12937.

Conforti, L., Adalbert, R., and Coleman, M.P. (2007). Neuronal death: where does the end begin? Trends Neurosci. *30*, 159–166. https://doi.org/10.1016/j.tins.2007.02.004.

Cooper, M.L., Pasini, S., Lambert, W.S., D'Alessandro, K.B., Yao, V., Risner, M.L., and Calkins, D.J. (2020). Redistribution of metabolic resources through astrocyte networks mitigates neurodegenerative stress. Proc. Natl. Acad. Sci. U S A *117*, 18810–18821. https://doi.org/10.1073/pnas.2009425117.

Cueva Vargas, J.L., Osswald, I.K., Unsain, N., Aurousseau, M.R., Barker, P.A., Bowie, D., and Di Polo, A. (2015). Soluble tumor necrosis factor Alpha promotes retinal ganglion cell death in glaucoma via calcium-permeable AMPA receptor activation. J. Neurosci. *35*, 12088–12102. https://doi.org/10.1523/JNEUROSCI.1273-15.2015.

Das, M.M., and Svendsen, C.N. (2015). Astrocytes show reduced support of motor neurons with aging that is accelerated in a rodent model of ALS. Neurobiol. Aging *36*, 1130–1139. https://doi.org/10.1016/j.neurobiolaging.2014.09.020.

De Leo, M.G., Staiano, L., Vicinanza, M., Luciani, A., Carissimo, A., Mutarelli, M., Di Campli, A., Polishchuk, E., Di Tullio, G., Morra, V., et al. (2016). Autophagosome-lysosome fusion triggers a lysosomal response mediated by TLR9 and controlled by OCRL. Nat. Cell Biol. *18*, 839–850. https://doi.org/10.1038/ncb3386.

Diaz-Amarilla, P., Olivera-Bravo, S., Trias, E., Cragnolini, A., Martinez-Palma, L., Cassina, P., Beckman, J., and Barbeito, L. (2011). Phenotypically aberrant astrocytes that promote motoneuron damage in a model of inherited amyotrophic lateral sclerosis. Proc. Natl. Acad. Sci. U S A *108*, 18126–18131. https://doi.org/10.1073/pnas.1110689108.

Escartin, C., Galea, E., Lakatos, A., O'Callaghan, J.P., Petzold, G.C., Serrano-Pozo, A., Steinhauser, C., Volterra, A., Carmignoto, G., Agarwal, A., et al. (2021). Reactive astrocyte nomenclature, definitions, and future directions. Nat. Neurosci. *24*, 312–325. https://doi.org/10.1038/s41593-020-00783-4.

Fan, B.J., and Wiggs, J.L. (2010). Glaucoma: genes, phenotypes, and new directions for therapy. J. Clin. Invest. *120*, 3064–3072. https://doi.org/10.1172/JCI43085.

Fligor, C.M., Huang, K.C., Lavekar, S.S., VanderWall, K.B., and Meyer, J.S. (2020). Differentiation of retinal organoids from human pluripotent stem cells. Methods Cell Biol. *159*, 279–302. https://doi.org/10.1016/bs.mcb.2020.02.005.

Fominykh, V., Vorobyeva, A., Onufriev, M.V., Brylev, L., Zakharova, M.N., and Gulyaeva, N.V. (2018). Interleukin-6, S-nitrosothiols, and neurodegeneration in different central nervous system demyelinating disorders: is there a relationship? J. Clin. Neurol. *14*, 327–332. https://doi.org/10.3988/jcn.2018.14.3.327.

R Formichella, C., Abella, S.K., Sims, S.M., Cathcart, H.M., and Sappington, R.M. (2014). Astrocyte reactivity: a biomarker for retinal ganglion cell health in retinal neurodegeneration. J. Clin. Cell. Immunol. *05*, 188. https://doi.org/10.4172/2155-9899.1000188.

Gomes, C., Cunha, C., Nascimento, F., Ribeiro, J.A., Vaz, A.R., and Brites, D. (2019). Cortical neurotoxic astrocytes with early ALS pathology and miR-146a deficit replicate gliosis markers of symptomatic SOD1G93A mouse model. Mol. Neurobiol. *56*, 2137–2158. https://doi.org/10.1007/s12035-018-1220-8.

Gruber, H.E., Ingram, J.A., Davis, D.E., and Hanley, E.N., Jr. (2009). Increased cell senescence is associated with decreased cell proliferation in vivo in the degenerating human annulus. Spine J. *9*, 210–215. https://doi.org/10.1016/j.spinee.2008.01.012.

Guttenplan, K.A., Stafford, B.K., El-Danaf, R.N., Adler, D.I., Munch, A.E., Weigel, M.K., Huberman, A.D., and Liddelow, S.A. (2020). Neurotoxic reactive astrocytes drive neuronal death after retinal injury. Cell Rep. *31*, 107776. https://doi.org/10.1016/j.celrep.2020.107776.

Hartwick, A.T.E. (2001). Beyond intraocular pressure: neuroprotective strategies for future glaucoma therapy. Optom. Vis. Sci. *78*, 85–94. https://doi.org/10.1097/00006324-200102000-00008.

Hodge, R.D., Bakken, T.E., Miller, J.A., Smith, K.A., Barkan, E.R., Graybuck, L.T., Close, J.L., Long, B., Johansen, N., Penn, O., et al. (2019). Conserved cell types with divergent features in human versus mouse cortex. Nature *573*, 61–68. https://doi.org/10.1038/s41586-019-1506-7.

Hol, E.M., and Pekny, M. (2015). Glial fibrillary acidic protein (GFAP) and the astrocyte intermediate filament system in diseases of the central nervous system. Curr. Opin. Cell Biol. *32*, 121–130. https://doi.org/10.1016/j.ceb.2015.02.004.

Inagaki, S., Kawase, K., Funato, M., Seki, J., Kawase, C., Ohuchi, K., Kameyama, T., Ando, S., Sato, A., Morozumi, W., et al. (2018). Effect of timolol on optineurin aggregation in transformed induced pluripotent stem cells derived from patient with familial glaucoma. Invest. Ophthalmol. Vis. Sci. *59*, 2293–2304. https://doi.org/10.1167/iovs.17-22975.

Ko, K.W., Milbrandt, J., and DiAntonio, A. (2020). SARM1 acts downstream of neuroinflammatory and necroptotic signaling to induce axon degeneration. J. Cell Biol. *219*. https://doi.org/10.1083/jcb.201912047.

Krencik, R., and Zhang, S.C. (2011). Directed differentiation of functional astroglial subtypes from human pluripotent stem cells. Nat. Protoc. *6*, 1710–1717. https://doi.org/10.1038/nprot.2011.405.

Liddelow, S.A., and Barres, B.A. (2017). Reactive astrocytes: production, function, and therapeutic potential. Immunity *46*, 957–967. https://doi.org/10.1016/j.immuni.2017.06.006.

Mac Nair, C.E., and Nickells, R.W. (2015). Neuroinflammation in glaucoma and optic nerve damage. Prog. Mol. Biol. Transl. Sci. *134*, 343–363. https://doi.org/10.1016/bs.pmbts.2015.06.010.

Marchetto, M.C., Muotri, A.R., Mu, Y., Smith, A.M., Cezar, G.G., and Gage, F.H. (2008). Non-cell-autonomous effect of human SOD1 G37R astrocytes on motor neurons derived from human embryonic stem cells. Cell Stem Cell *3*, 649–657. https://doi.org/10.1016/j.stem.2008.10.001.

Martinez-Cue, C., and Rueda, N. (2020). Cellular senescence in neurodegenerative diseases. Front. Cell. Neurosci. *14*, 16. https://doi.org/10.3389/fncel.2020.00016.

Meyer, K., Ferraiuolo, L., Miranda, C.J., Likhite, S., McElroy, S., Renusch, S., Ditsworth, D., Lagier-Tourenne, C., Smith, R.A., Ravits, J., et al. (2014). Direct conversion of patient fibroblasts demonstrates non-cell autonomous toxicity of astrocytes to motor neurons in familial and sporadic ALS. Proc. Natl. Acad. Sci. U S A *111*, 829–832. https://doi.org/10.1073/pnas.1314085111.

Michetti, F., D'Ambrosi, N., Toesca, A., Puglisi, M.A., Serrano, A., Marchese, E., Corvino, V., and Geloso, M.C. (2019). The S100B story: from biomarker to active factor in neural injury. J. Neurochem. *148*, 168–187. https://doi.org/10.1111/jnc.14574.

Minegishi, Y., Iejima, D., Kobayashi, H., Chi, Z.L., Kawase, K., Yamamoto, T., Seki, T., Yuasa, S., Fukuda, K., and Iwata, T. (2013). Enhanced optineurin E50K-TBK1 interaction evokes protein insolubility and initiates familial primary open-angle glaucoma. Hum. Mol. Genet. *22*, 3559–3567. https://doi.org/10.1093/hmg/ddt210.

Netzahualcoyotzi, C., and Tapia, R. (2015). Degeneration of spinal motor neurons by chronic AMPA-induced excitotoxicity in vivo and protection by energy substrates. Acta Neuropathol. Commun. *3*, 27. https://doi.org/10.1186/s40478-015-0205-3.

Oberheim, N.A., Takano, T., Han, X., He, W., Lin, J.H.C., Wang, F., Xu, Q., Wyatt, J.D., Pilcher, W., Ojemann, J.G., et al. (2009). Uniquely hominid features of adult human astrocytes. J. Neurosci. *29*, 3276–3287. https://doi.org/10.1523/JNEUROSCI.4707-08.2009.

Ohlemacher, S.K., Iglesias, C.L., Sridhar, A., Gamm, D.M., and Meyer, J.S. (2015). Generation of highly enriched populations of optic vesicle-like retinal cells from human pluripotent stem cells. Curr. Protoc. Stem Cell Biol. *32*, 1H 8 1–1H 8 20. https://doi.org/10.1002/9780470151808.sc01h08s32.

Ohlemacher, S.K., Sridhar, A., Xiao, Y., Hochstetler, A.E., Sarfarazi, M., Cummins, T.R., and Meyer, J.S. (2016). Stepwise differentiation of retinal ganglion cells from human pluripotent stem cells enables analysis of glaucomatous neurodegeneration. Stem Cell. *34*, 1553–1562. https://doi.org/10.1002/stem.2356.

Ohlmann, A., Scholz, M., Goldwich, A., Chauhan, B.K., Hudl, K., Ohlmann, A.V., Zrenner, E., Berger, W., Cvekl, A., Seeliger, M.W., and Tamm, E.R. (2005). Ectopic norrin induces growth of ocular capillaries and restores normal retinal angiogenesis in Norrie disease mutant mice. J. Neurosci. *25*, 1701–1710. https://doi.org/10.1523/jneurosci.4756-04.2005.

Paixao, S., and Klein, R. (2010). Neuron-astrocyte communication and synaptic plasticity. Curr. Opin. Neurobiol. *20*, 466–473. https://doi.org/10.1016/j.conb.2010.04.008.

Peng, Y.R., Shekhar, K., Yan, W., Herrmann, D., Sappington, A., Bryman, G.S., van Zyl, T., Do, M.T.H., Regev, A., and Sanes, J.R. (2019). Molecular classification and comparative taxonomics of foveal and peripheral cells in primate retina. Cell *176*, 1222–1237.e22. https://doi.org/10.1016/j.cell.2019.01.004.

Perigolo-Vicente, R., Ritt, K., Pereira, M.R., Torres, P.M.M., Paes-de-Carvalho, R., and Giestal-de-Araujo, E. (2013). IL-6 treatment increases the survival of retinal ganglion cells in vitro: the role of adenosine A1 receptor. Biochem. Biophys. Res. Commun. *430*, 512–518. https://doi.org/10.1016/j.bbrc.2012.12.004.

Phatnani, H., and Maniatis, T. (2015). Astrocytes in neurodegenerative disease: table 1. Cold Spring Harb. Perspect. Biol. *7*. https://doi.org/10.1101/cshperspect.a020628.

Phuagkhaopong, S., Ospondpant, D., Kasemsuk, T., Sibmooh, N., Soodvilai, S., Power, C., and Vivithanaporn, P. (2017). Cadmium-induced IL-6 and IL-8 expression and release from astrocytes are mediated by MAPK and NF-κB pathways. Neurotoxicology *60*, 82–91. https://doi.org/10.1016/j.neuro.2017.03.001.

Quigley, H.A. (2011). Glaucoma. Lancet *377*, 1367–1377. https://doi.org/10.1016/S0140-6736(10)61423-7.

Ramirez-Jarquin, U.N., Rojas, F., van Zundert, B., and Tapia, R. (2017). Chronic infusion of SOD1(G93A) astrocyte-secreted factors induces spinal motoneuron degeneration and neuromuscular

dysfunction in healthy rats. J. Cell. Physiol. *232*, 2610–2615. https://doi.org/10.1002/jcp.25827.

Sappington, R.M., Chan, M., and Calkins, D.J. (2006). Interleukin-6 protects retinal ganglion cells from pressure-induced death. Invest. Ophthalmol. Vis. Sci. *47*, 2932–2942. https://doi.org/10.1167/iovs.05-1407.

Sears, N.C., Boese, E.A., Miller, M.A., and Fingert, J.H. (2019). Mendelian genes in primary open angle glaucoma. Exp. Eye Res. *186*, 107702. https://doi.org/10.1016/j.exer.2019.107702.

Sena, D.F., Finzi, S., Rodgers, K., Del Bono, E., Haines, J.L., and Wiggs, J.L. (2004). Founder mutations of CYP1B1 gene in patients with congenital glaucoma from the United States and Brazil. J. Med. Genet. *41*, e6. https://doi.org/10.1136/jmg.2003.010777.

Sharma, T.P., Wiley, L.A., Whitmore, S.S., Anfinson, K.R., Cranston, C.M., Oppedal, D.J., Daggett, H.T., Mullins, R.F., Tucker, B.A., and Stone, E.M. (2017). Patient-specific induced pluripotent stem cells to evaluate the pathophysiology of TRNT1-associated Retinitis pigmentosa. Stem Cell Res. *21*, 58–70. https://doi.org/10.1016/j.scr.2017.03.005.

Shim, M.S., Takihara, Y., Kim, K.Y., Iwata, T., Yue, B.Y.J.T., Inatani, M., Weinreb, R.N., Perkins, G.A., and Ju, W.K. (2016). Mitochondrial pathogenic mechanism and degradation in optineurin E50K mutation-mediated retinal ganglion cell degeneration. Sci. Rep. *6*, 33830. https://doi.org/10.1038/srep33830.

Shinozaki, Y., and Koizumi, S. (2021). Potential roles of astrocytes and Muller cells in the pathogenesis of glaucoma. J. Pharmacol. Sci. *145*, 262–267. https://doi.org/10.1016/j.jphs.2020.12.009.

Slowicka, K., Vereecke, L., and van Loo, G. (2016). Cellular functions of optineurin in health and disease. Trends Immunol. *37*, 621–633. https://doi.org/10.1016/j.it.2016.07.002.

Sofroniew, M.V., and Vinters, H.V. (2010). Astrocytes: biology and pathology. Acta Neuropathol. *119*, 7–35. https://doi.org/10.1007/s00401-009-0619-8.

Sun, W., Cornwell, A., Li, J., Peng, S., Osorio, M.J., Aalling, N., Wang, S., Benraiss, A., Lou, N., Goldman, S.A., and Nedergaard, M. (2017). SOX9 is an astrocyte-specific nuclear marker in the adult brain outside the neurogenic regions. J. Neurosci. *37*, 4493–4507. https://doi.org/10.1523/JNEUROSCI.3199-16.2017.

Syc-Mazurek, S.B., and Libby, R.T. (2019). Axon injury signaling and compartmentalized injury response in glaucoma. Prog. Retin. Eye Res. *73*, 100769. https://doi.org/10.1016/j.preteyeres.2019.07.002.

Teotia, P., Van Hook, M.J., Wichman, C.S., Allingham, R.R., Hauser, M.A., and Ahmad, I. (2017). Modeling glaucoma: retinal ganglion cells generated from induced pluripotent stem cells of patients with SIX6 risk allele show developmental abnormalities. Stem Cell. *35*, 2239–2252. https://doi.org/10.1002/stem.2675.

Tripathi, P., Rodriguez-Muela, N., Klim, J.R., de Boer, A.S., Agrawal, S., Sandoe, J., Lopes, C.S., Ogliari, K.S., Williams, L.A., Shear, M., et al. (2017). Reactive astrocytes promote ALS-like degeneration and intracellular protein aggregation in human motor neurons by disrupting autophagy through TGF-β1. Stem Cell Rep. *9*, 667–680. https://doi.org/10.1016/j.stemcr.2017.06.008.

VanderWall, K.B., Huang, K.C., Pan, Y., Lavekar, S.S., Fligor, C.M., Allsop, A.R., Lentsch, K.A., Dang, P., Zhang, C., Tseng, H.C., et al. (2020). Retinal ganglion cells with a glaucoma OPTN(E50K) mutation exhibit neurodegenerative phenotypes when derived from three-dimensional retinal organoids. Stem Cell Rep. *15*, 52–66. https://doi.org/10.1016/j.stemcr.2020.05.009.

VanderWall, K.B., Vij, R., Ohlemacher, S.K., Sridhar, A., Fligor, C.M., Feder, E.M., Edler, M.C., Baucum, A.J., Cummins, T.R., and Meyer, J.S. (2019). Astrocytes regulate the development and maturation of retinal ganglion cells derived from human pluripotent stem cells. Stem Cell Rep. *12*, 201–212. https://doi.org/10.1016/j.stemcr.2018.12.010.

Vecino, E., Rodriguez, F.D., Ruzafa, N., Pereiro, X., and Sharma, S.C. (2016). Glia-neuron interactions in the mammalian retina. Prog. Retin. Eye Res. *51*, 1–40. https://doi.org/10.1016/j.preteyeres.2015.06.003.

Verheijen, J., Van den Bossche, T., van der Zee, J., Engelborghs, S., Sanchez-Valle, R., Llado, A., Graff, C., Thonberg, H., Pastor, P., Ortega-Cubero, S., et al. (2016). A comprehensive study of the genetic impact of rare variants in SORL1 in European early-onset Alzheimer's disease. Acta Neuropathol. *132*, 213–224. https://doi.org/10.1007/s00401-016-1566-9.

Whitmore, A.V., Libby, R.T., and John, S.W. (2005). Glaucoma: thinking in new ways-a role for autonomous axonal self-destruction and other compartmentalised processes? Prog. Retin. Eye Res. *24*, 639–662. https://doi.org/10.1016/j.preteyeres.2005.04.004.

Yin, R.H., Yu, J.T., and Tan, L. (2015). The role of SORL1 in alzheimer's disease. Mol. Neurobiol. *51*, 909–918. https://doi.org/10.1007/s12035-014-8742-5.

Yoshii, Y., Otomo, A., Pan, L., Ohtsuka, M., and Hadano, S. (2011). Loss of glial fibrillary acidic protein marginally accelerates disease progression in a SOD1(H46R) transgenic mouse model of ALS. Neurosci. Res. *70*, 321–329. https://doi.org/10.1016/j.neures.2011.03.006.

Zhang, C.C., Xing, A., Tan, M.S., Tan, L., and Yu, J.T. (2016a). The role of MAPT in neurodegenerative diseases: genetics, mechanisms and therapy. Mol. Neurobiol. *53*, 4893–4904. https://doi.org/10.1007/s12035-015-9415-8.

Zhang, Y., Sloan, S.A., Clarke, L.E., Caneda, C., Plaza, C.A., Blumenthal, P.D., Vogel, H., Steinberg, G.K., Edwards, M.S., Li, G., et al. (2016b). Purification and characterization of progenitor and mature human astrocytes reveals transcriptional and functional differences with mouse. Neuron *89*, 37–53. https://doi.org/10.1016/j.neuron.2015.11.013.